Structural Transformation from Trinuclear Linear to Tetranuclear Cubane Heterobimetallic Selenium Compounds. Structure and Optical Linearities of $[Et_4N]_2[(\mu\text{-}WSe_4)(CuCl)_2]$

Shu-Lei Liu[a], Taike Duan[a], Qian-Feng Zhang[a,b], and Wa-Hung Leung[c]

[a] Institute of Molecular Engineering and Applied Chemistry, Anhui University of Technology, Ma'anshan, Anhui 243002, P. R. China
[b] State Key Laboratory of Coordination Chemistry, Nanjing University, Nanjing 210009, P. R. China
[c] Department of Chemistry, The Hong Kong University of Science and Technology, Clear Water Bay, Kowloon, Hong Kong, P. R. China

Reprint requests to Dr. Qian-Feng Zhang and Prof. Wa-Hung Leung. Fax: +86-555-2312041. E-mail: zhangqf@ahut.edu.cn and chleung@ust.hk

Z. Naturforsch. **2009**, *64b,* 209 – 214; received September 22, 2008

Reactions of $[Et_4N]_2[WSe_4]$ with two equivalents of [CuX] powder gave trinuclear linear compounds $[Et_4N]_2[(\mu\text{-}WSe_4)(CuX)_2]$ (X = Cl **1**, Br **2**). Treatment of **1** or **2** with PPh_3 in CH_2Cl_2 resulted in the formation of tetranuclear cubane-like compounds $(\mu_3\text{-}X)(\mu_3\text{-}WSe_4)(CuPPh_3)_3$ (X = Cl **3**, Br **4**). The structures of the heterobimetallic selenium compounds **1** and **4**·MeCN were confirmed by single-crystal X-ray diffraction. The nonlinear optical properties of **1** were investigated at λ = 532 nm with a pulse width of 7 ns.

Key words: Synthesis, Crystal Structure, Heteroselenometallic Compound, Nonlinear Optical Properties

Introduction

The chemistry of the heteroselenometallic compounds containing anions $[MSe_4]^{2-}$ (M = Mo, W) has received attention owing to their structures and nonlinear optical (NLO) properties in recent years [1]. Compared with heterothiometallic compounds, it is reasonably speculated that, similar to their sulfur counterparts, selenium-containing compounds may also possess large NLO properties [2, 3]. An important reason is that the heavy atom effect may result in effective improvement of NLO properties [4]. Another important reason is that selenium-containing compounds have important applications as precursors for low band gap semiconductors and in nonlinear optics [5]. In this connection, we set out to isolate new heteroselenometallic compounds from reactions between tetraselenometalate anions and coinage metal cations, and further to investigate the structure-property relationship of this class of compounds. A number of heteroselenometallic compounds have been successfully isolated to date. Their structural types include linear, butterfly, cubane, incomplete cubane, coplanar T-frame and open cross-frame, crown, cage, and pin-wheel shapes [6 – 16]. Among these heteroselenometallic compounds, the variation of structural types mainly depends on the number of coinage metal atoms bound to the tetrahedral $[MSe_4]^{2-}$ moiety, which probably influences the NLO properties of the compounds [14, 16]. Herein, we report the syntheses of trinuclear linear compounds $[Et_4N]_2[(\mu\text{-}WSe_4)(CuX)_2]$ (X = Cl **1**, Br **2**) and their structural transformation to tetranuclear cubane-like compounds $(\mu_3\text{-}X)(\mu_3\text{-}WSe_4)(CuPPh_3)_3$ (X = Cl **3**, Br **4**). Their structures and spectroscopic properties along with NLO properties were investigated.

Experimental Section

General

All manipulations were conducted using Schlenk techniques under an atmosphere of nitrogen. All reagents, unless otherwise stated, were purchased as analysis grade and were used without further purification. $[Et_4N]_2[WSe_4]$ was prepared by a modification of the literature method [17]. Infrared spectra were recorded on a Digilab FTS-40 spectrophotometer with use of pressed KBr pellets. Electronic spectra were obtained on a Hitachi U-3410 spectrophotometer. All elemental analyses were carried out using a Perkin-Elmer 2400 CHN analyzer.

Syntheses

*$[Et_4N]_2[(\mu\text{-}WSe_4)(CuCl)_2]$ (**1**)*

To a solution of $[Et_4N]_2[WSe_4]$ (190 mg, 0.25 mmol) in DMF (15 mL) was added a suspension of CuCl (50 mg, 0.50 mmol) in MeCN (3 mL). The mixture was stirred at r. t. for 1 h, during which time the color gradually changed from purple to red and a precipitate formed. The precipitate was re-dissolved upon addition of 1 mL 2,6-dimethylpyridine to the reaction mixture. The resulting red solution was stirred for additional 0.5 h and subsequently filtered to remove small amounts of a red precipitate. Slow addition of THF induced the crystallization of **1** as red blocks suitable for X-ray analysis. Yield: 134 mg (56 %). – Anal. for $C_{16}H_{40}N_2Cl_2Cu_2Se_4W$: calcd. C 20.1, H 4.21, N 2.92; found C 20.2, H 4.17, N 2.90. – UV/Vis (DMF, nm): λ = 361(sh), 484(br).

*$[Et_4N]_2[(\mu\text{-}WSe_4)(CuBr)_2]$ (**2**)*

Compound **2** was prepared similarly as described for **1** using CuBr (72 mg, 0.5 mmol) instead of CuCl. Red microcrystals were obtained in a yield of 59 % (155 mg). – UV/Vis (DMF): λ = 364(sh), 487(br) nm. – Anal. for $C_{16}H_{40}N_2Br_2Cu_2Se_4W$: calcd. C 18.4, H 3.85, N 2.68; found C 18.2, H 3.88, N 2.65.

*$(\mu_3\text{-}X)(\mu_3\text{-}WSe_4)(CuPPh_3)_3$(X = Cl **3**, Br **4**)*

To a slurry of **1** (96 mg, 0.10 mmol) or **2** (105 mg, 0.10 mmol) in DMF (3 mL) was added a solution of PPh_3 (157 mg, 0.60 mmol) in CH_2Cl_2 (15 mL), and the mixture was stirred for 4 h at r. t. The resulting orange-red solution was filtered to remove small amounts of an orange precipitate. Orange-red crystals of **3** or **4** were obtained by layering the filtrate with MeCN. For **3**: Yield: 114 mg (51 %). – UV/Vis (CH_2Cl_2): λ = 325 (s), 459 (br), 498 (sh) nm. – Anal. for $C_{54}H_{45}P_3ClCu_3Se_4W\cdot(C_2H_3N)$: calcd. C 43.3, H 3.11, N 0.90; found C 43.1, H 3.13, N 0.88. For **4**: Yield: 136 mg (57 %). – UV/Vis (CH_2Cl_2): λ = 321 (s), 455 (br), 502 (sh) nm. – Anal. for $C_{54}H_{45}P_3BrCu_3Se_4W\cdot(C_2H_3N)$: calcd. C 42.1, H 3.03, N 0.88; found C 41.8, H 3.01, N 0.87.

Crystal structure determination

Single crystals of **1** ($0.22 \times 0.16 \times 0.12$ mm^3) and **4**·MeCN ($0.24 \times 0.17 \times 0.10$ mm^3) were mounted in random orientation on glass fibers. Diffraction data were collected on a Bruker SMART Apex CCD diffractometer with MoK_α radiation (λ = 0.71073 Å) at 296 K using an ω scan mode. The collected frames were processed with the software SAINT [18]. The data were corrected for absorption using the program SADABS [19]. Structures were solved by Direct Methods and refined by full-matrix least-squares on F^2 using the SHELXTL software package [20]. All non-hydrogen atoms were refined anisotropically. The positions of all hydrogen atoms were generated geometrically (C_{sp^3}–H = 0.96 and C_{sp^2}–H = 0.93 Å) and included in the structure factor calculations with assigned isotropic displacement parameters but were not refined. The MeCN solvent molecule in **4**·MeCN was refined isotropically with the hydrogen atoms. Crystal data, data collection parameters and details of the structure refinement are given in Table 1.

Table 1. Crystal data, data collection parameters and details of the structure refinement.

Complex	**1**	**4**·MeCN
Empirical formula	$C_{16}H_{40}N_2Cl_2Cu_2Se_4W$	$C_{56}H_{48}NP_3BrCu_3Se_4W$
Formula weight	958.17	1598.085
Color, habit	red, block	orange-red, block
Crystal size, mm^3	0.23×0.16×0.12	0.24×0.17×0.10
Crystal system	monoclinic	rhombohedral
Space group	$P2_1/n$	$R\bar{3}$
a, Å	7.4856(1)	15.8058(2)
b, Å	13.5186(2)	15.8058(2)
c, Å	29.0547(5)	23.9394(7)
α, deg	90	90
β, deg	92.864(1)	90
γ, deg	90	120
Volume, Å^3	2936.51(8)	5179.37(18)
Z	4	3
Density (calc.), g cm^{-3}	2.17	1.54
Absorption coefficient, mm^{-1}	10.5	5.4
Temperature, K	296(2)	296(2)
F(000) e	1808	2304
Radiation	— MoK_α (λ = 0.71073 Å) —	
Reflections collected	28928	15376
– independent	6728	4740
R_{int}	0.052	0.026
Refls [$I \geq 2\sigma(I)$]	4823	4135
Parameters refined	252	207
Final $R1/wR2$ (all data)[a]	0.062/0.076	0.048/0.101
Weighting scheme;	0.0373/0.5140	0.0629/3.2569
– param. a/b		
Goodness of fit (GoF)[b]	1.02	1.10
x (Flack)	–	0.00 (0)
Final difference peaks, e Å^{-3}	+0.96, −0.85	+1.04, −1.17

[a] $R1 = \Sigma||F_o| - |F_c||/\Sigma|F_o|$; $wR2 = [\Sigma w(F_o^2 - F_c^2)^2/\Sigma w(F_o^2)^2]^{1/2}$, $w = 1/[\sigma^2(F_o^2) + (aP)^2 + bP]$ where $P = (F_o^2 + 2F_c^2)/3$; [b] GoF = $[\Sigma w(F_o^2 - F_c^2)^2/(N_{obs} - N_{param})]^{1/2}$.

CCDC 703019/703020 contain the supplementary crystallographic data for this paper. These data can be obtained free of charge from The Cambridge Crystallographic Data Centre *via* www.ccdc.cam.ac.uk/data_request/cif.

Optical measurements

A DMF solution of 2.15×10^{-3} mol dm^{-3} of compound **1** was placed in a 1 mm quartz cuvette for optical measurements. The optical limiting characteristics along with nonlinear absorption and refraction was investigated with a linearly polarized laser light (λ = 532 nm, pulse width = 7 ns) generated from a Q-switched and frequency-doubled Nd : YAG

Table 2. Selected bond lengths (Å) and bond angles (deg) for $[Et_4N]_2[(\mu\text{-}WSe_4)(CuCl)_2]$ (**1**).

W(1)–Se(1)	2.3409(6)	W(1)–Se(2)	2.3385(6)
W(1)–Se(3)	2.3399(6)	W(1)–Se(4)	2.3366(6)
Cu(1)–Se(1)	2.3348(9)	Cu(1)–Se(2)	2.3337(9)
Cu(2)–Se(3)	2.3396(8)	Cu(2)–Se(4)	2.3382(10)
Cu(1)–Cl(1)	2.1599(16)	Cu(2)–Cl(2)	2.1668(17)
W(1)–Cu(1)	2.6607(7)	W(1)–Cu(2)	2.6887(7)
Se(2)–W(1)–Se(1)	110.39(2)	Se(3)–W(1)–Se(1)	110.08(2)
Se(4)–W(1)–Se(1)	108.80(3)	Se(2)–W(1)–Se(3)	108.29(2)
Se(4)–W(1)–Se(2)	109.46(2)	Se(4)–W(1)–Se(3)	109.82(2)
Cu(1)–Se(1)–W(1)	69.37(2)	Cu(1)–Se(2)–W(1)	69.43(2)
Cu(2)–Se(3)–W(1)	70.14(2)	Cu(2)–Se(4)–W(1)	70.22(2)
Cl(1)–Cu(1)–Se(1)	124.69(5)	Cl(1)–Cu(1)–Se(2)	124.52(5)
Se(2)–Cu(1)–Se(1)	110.77(3)	Se(4)–Cu(2)–Se(3)	109.77(3)
Cl(2)–Cu(2)–Se(3)	124.29(6)	Cl(2)–Cu(2)–Se(4)	125.92(6)

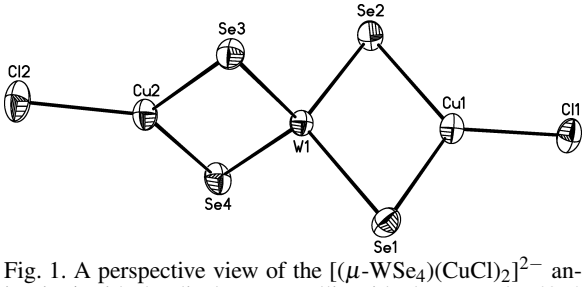

Fig. 1. A perspective view of the $[(\mu\text{-}WSe_4)(CuCl)_2]^{2-}$ anion in **1** with the displacement ellipsoids drawn at the 40 % probability level.

laser. The spatial profiles of the optical pulses were nearly Gaussian. The laser beam was focused with a 25 cm focal-length focusing mirror. The radius of the laser beam waist was measured to be 30 ± 5 μm (half-width at $1/e^2$ maximum in irradiance). The incident and transmitted pulse energy were measured simultaneously by two Laser Precision detectors (RjP-735 energy probes) communicating to a computer *via* an IEEE interface [21].

Results and Discussion

Treatment of $[Et_4N]_2[WSe_4]$ in DMF with two equivalents of CuCl in CH_3CN suspension resulted in a color change from purple to red and a red precipitate. Upon addition of 2,6-dimethylpyridine, the red precipitate was redissolved to give a clear red solution, from which red block-shaped crystals of $[Et_4N]_2[(\mu\text{-}WSe_4)(CuCl)_2]$ (**1**) were obtained in 56 % yield. The bromide analog $[Et_4N]_2[(\mu\text{-}WSe_4)(CuBr)_2]$ (**2**) was isolated from CuBr powder under similar reaction conditions. It should be noted that bulk 2,6-dimethylpyridine acts as a co-solvent instead of a ligand in the present system. Addition of a small amount of 2,6-dimethylpyridine increases the solubility of the solid reactants, resulting in the isolation of crystalline products in moderate yields. A similar synthetic route was used to prepare the cyanide-bridged three-dimensional framework cluster compound $\{[Et_4N]_2[(\mu_4\text{-}WSe_4)Cu_4(CN)_4]\}_n$ [12] and crown-like cluster compounds $[Et_4N]_4[(\mu_5\text{-}WSe_4)(CuX)_5(\mu\text{-}X)_2]$ (X = Cl, Br) [15].

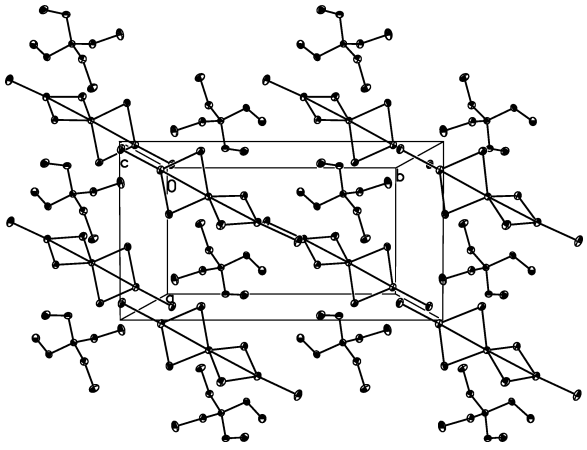

Fig. 2. Packing arrangement of $[Et_4N]_2[(\mu\text{-}WSe_4)(CuCl)_2]$ (**1**), showing well separated cations and anions.

The structure of **1** was confirmed by an X-ray diffraction study. The structure consists of well separated cations and anions, as shown in Fig. 2 as a view of the cell packing. The $[Et_4N]^+$ cations have normal bond lengths and angles, which will not be discussed here. The $[(\mu\text{-}WSe_4)(CuCl)_2]^{2-}$ anion is shown in Fig. 1, and selected bond lengths and angles are given in Table 2. The trinuclear linear structure of the anion comprises two CuCl fragments ligating at opposite edges of the tetrahedral $[WSe_4]^{2-}$ moiety. Similar structures of heteroselenometallic compounds such as anionic $[(\mu\text{-}WSe_4)(CuCN)_2]^{2-}$ [8] and neutral $[(\mu\text{-}WSe_4)(MPR_3)_2]$ (M = Ag, Au; R_3 = Ph_3, Me_2Ph) [6, 22, 23] have been previously reported. The tungsten atom in **1** has an essentially tetrahedral coordination geometry with the Se–W–Se angles ranging from 108.29(2) to 110.39(2)°. The average W–Se bond length of 2.3390(6) Å is comparable to those in related heteroselenometallic compounds, but is obviously longer than those in free $[WSe_4]^{2-}$ as expected. The geometry around the copper atoms is distorted trigonal planar with an average Se–Cu–Se angle of 110.27(3)°. The W–Cu distances are 2.6607(7) and 2.6887(7) Å, which are shorter than those in related heteroselenometallic compounds, indicative of a weak W^{VI}–Cu^{I} interaction in **1**. There is a small distortion

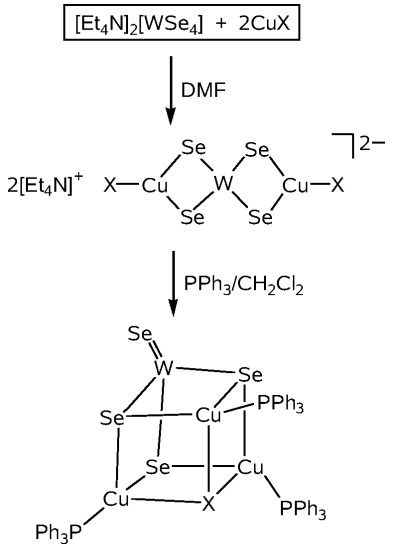

Scheme 1. Reactions of structural change from trinuclear linear to tetranuclear cubane compounds.

from ideal D_{2d} symmetry of the anion as a result of bending along the Cl–Cu–W–Cu–Cl axis that results in a Cu–W–Cu angle of 177.43(2)° and W–Cu–Cl angles of 176.90(6) and 177.36(6)°. The terminal Cu–Cl bond lengths are 2.1599(16) and 2.1668(17) Å, which agree well with those in $[Et_4N]_4[(\mu_5\text{-}WSe_4)(CuCl)_5(\mu\text{-}Cl)_2]$ (2.204(3) and 2.215(3) Å) [15].

When compounds **1** and **2** were reacted with PPh_3 in a mixed CH_2Cl_2/DMF solvent, the cubane-like compounds $(\mu_3\text{-}X)(\mu_3\text{-}WSe_4)(CuPPh_3)_3$ (X = Cl **3**, Br **4**) were obtained (see Scheme 1). The reactions involve the substitution of halide by the strong σ donor PPh_3 and structure transformation from trinuclear linear to tetranuclear cubane-like. This observation together with our previous report on cluster skeleton change from cross plane to cubane suggests that the cubane-like compounds are structurally stabilized in the presence of PPh_3 and halide [12, 24].

Compound **4**·MeCN was characterized by single-crystal X-ray diffraction. A view of the structure of **4** is shown in Fig. 3, and selected bond lengths and angles are given in Table 3. The crystal structure consists of a neutral cubane-like cluster $(\mu_3\text{-Br})(\mu_3\text{-}WSe_4)(CuPPh_3)_3$ along with the solvent molecules. Both cubane-like compounds show bands at 2253 and 2251 cm^{-1} in their IR spectra, which are typical for the CN^- stretching absorbance, indicative of the MeCN solvent molecules in the structures. The molecular cluster of **4**·MeCN crystallized in the rhombo-

Table 3. Selected bond lengths (Å) and bond angles (deg) for $(\mu_3\text{-Br})(\mu_3\text{-}WSe_4)(CuPPh_3)_3$ (**4**·MeCN).

W(1)-Se(1)	2.2692(13)	W(1)-Se(2)	2.3722(7)
Cu(1)-Se(2)	2.3985(11)	Cu(1)-P(1)	2.230(2)
Cu(1)-Br(1)	2.7896(14)	W(1)-Cu(1)	2.7643(9)
Se(1)-W(1)-Se(2)	110.246(18)	Se(2)-W(1)-Se(2)$^{\#1}$	108.685(19)
W(1)-Se(2)-Cu(1)	70.82(3)	Cu(1)$^{\#2}$-Se(2)-Cu(1)	85.90(5)
Se(2)$^{\#2}$-Cu(1)-Se(2)	106.96(5)	P(1)-Cu(1)-Br(1)	110.14(7)
Se(2)#2-Cu(1)-Br(1)	98.63(4)	Se(2)-Cu(1)-Br(1)	98.62(4)
P(1)-Cu(1)-Se(2)$^{\#2}$	120.15(7)	P(1)-Cu(1)-Se(2)	118.41(7)
Cu(1)-Br(1)-Cu(1)$^{\#1}$	71.72(4)		

Symmetry operators: $^{\#1}$ $-x+y, -x+1, z$; $^{\#2}$ $-y+1, x-y+1, z$.

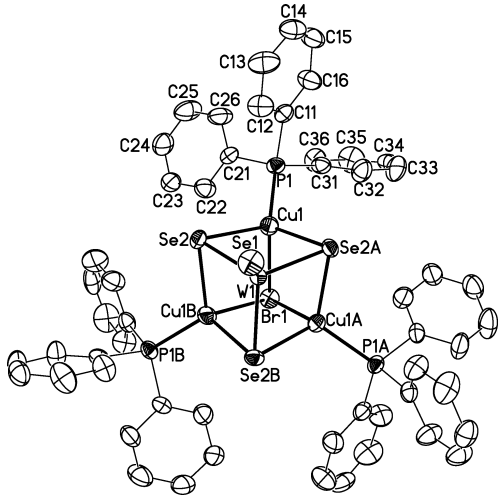

Fig. 3. Molecular structure of the cubane-like cluster compound $(\mu_3\text{-Br})(\mu_3\text{-}WSe_4)(CuPPh_3)_3$ (**4**) (displacement ellipsoids at the 40 % probability level).

hedral space group $R3$. The molecular structure possesses a crystallographic C_3 axis passing through the Se(1), W(1) and Br(1) atoms and the MeCN molecule. The neutral compound contains a highly distorted cubane-like $[WCu_3Se_3Br]$ cluster core and a PPh_3 ligand bound to each copper atom. The W–Se_b (bridging) distance of 2.3722(7) Å is obviously longer than the W–Se_t (terminal) distance of 2.2692(13) Å. The Se_t–W–Se_b angles are *ca.* 1.6° more obtuse than the Se_b–W–Se_b angles with an average Se–Cu–Se angle of 106.96(5)°. The average W–Cu distance of 2.7643(9) Å in **4**·MeCN is slightly longer than that of 2.6747(7) Å in **1**, but is still shorter than the sum of the van der Waals radii of tungsten and copper atoms, which suggests that minor interactions may exist between two metal atoms. The Cu–Br distance of 2.7896(14) Å in **4**·MeCN agrees well with that of 2.797(1) Å in $(\mu_3\text{-Br})(\mu_3\text{-}MoSe_4)(CuPPh_3)_3$ [24]. The average Cu–Br–Cu bond angle of 71.72(4)° in

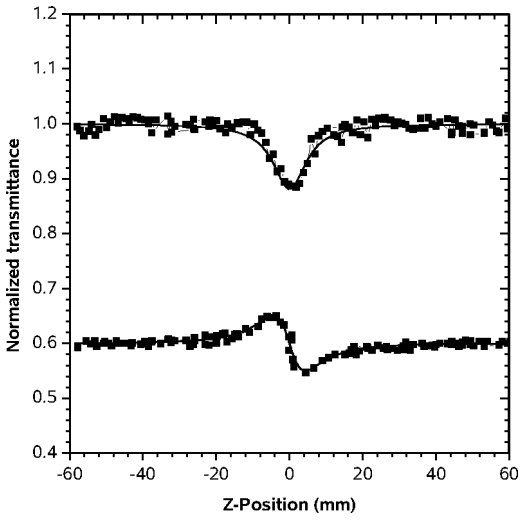

Fig. 4. *Z*-scan data of 2.15×10^{-3} M of **1** in DMF at 532 nm with I_o being 8.1×10^{10} W m^{-2} collected under the open aperture configuration showing NLO absorption (above) and obtained by dividing the normalized *Z*-scan data obtained under the closed aperture configuration (below) by the normalized *Z*-scan data in the up curve. The solid curves are theoretical fits based on *Z*-scan theoretical calculations.

4·MeCN deviates strongly from 90° as the standard cubane angle. This structural feature has also been observed in related cubane-like heteroselenometallic compounds [6, 24].

The electronic spectra of compounds **1** and **2** in DMF solution show intense absorption bands at 350–500 nm. The intense shoulder peaks at about 360–365 nm may be assigned to the Se → W charge transfer arising from the $[WSe_4]^{2-}$ moiety, whereas the weaker broad bands at about 485–490 nm may be ascribed to a relatively weak $[WSe_4]^{2-}$ to copper interaction [25]. It is interesting to note that the Se → W charge transfer transition peaks are *ca.* 40 nm blue shifted upon the structural change from trinuclear linear to tetranuclear cubane compounds, probably due to one terminal W=Se double bond being retained in the cubane-like compounds. Moreover, a comparison of the electronic spectra of the four compounds with that of the free $[WSe_4]^{2-}$ anion [26] suggests that all of the bands of $[WSe_4]^{2-}$ are shifted toward higher wavelength, thereby indicating a strong interaction between the $[WSe_4]^{2-}$ moiety and the copper atoms.

The NLO properties of compound **1** were investigated by using the *Z*-scan technique [21]. The nonlinear absorption component was evaluated under an open aperture configuration. Theoretical curves of transmittance against the *Z*-position, Eqs. 1 and 2, were fitted to the observed *Z*-scan data

$$T(Z) = \frac{1}{\pi 1/2_{q(Z)}} \int_{-\infty}^{\infty} \ln[1 + q(Z)] e^{-\tau^2} d\tau \qquad (1)$$

$$q(Z) = \alpha_2 I_i(Z) \frac{(1 - e^{-\alpha_0 L})}{\alpha_0} \qquad (2)$$

by varying the effective third-order NLO absorptivity α_2 value, where the experimentally measured α_0 (linear absorptivity), L (the optical path of the sample) and $I_i(z)$ (the on-axis irradiance at z position) were adopted. The solid line in Fig. 4 (above) is the theoretical curve calculated with $\alpha_2 = 6.11 \times 10^{-11}$ m W^{-1} for the concentration of 2.15×10^{-3} M of **1** in a DMF solution. The nonlinear refractive component plotted with the filled squares in Fig. 4 (below) was assessed by dividing the normalized *Z*-scan data obtained under the closed aperture configuration by the normalized *Z*-scan data obtained under the open aperture configuration. The valley and peak occur at about equal distances from the focus. It can be seen that the difference in valley-peak positions ΔZ_{V-P} is 7.3 mm and the difference between normalized transmittance values at valley and peak positions ΔT_{V-P} is 0.12 for **1**. These results suggest an effectively good third-order optical nonlinearity [24]. The solid curve is an eye guide for comparison where the effective nonlinear refractivity n_2 value estimated therefore is 4.18×10^{-13} esu for **1**. Comparing the NLO data of cluster compound **1** with that reported for M(W)/Cu(Ag)/S(Se) clusters [12–16, 27], it may be seen that the NLO behavior of compound **1** is comparable to those of polynuclear cluster compounds. The negative value of nonlinear refraction in **1** indicates that there are self-defocusing effects in NLO behavior of the crown-like cluster compound, which is obviously different from that of cubane-like cluster compounds that show self-focusing effects of nonlinear refraction [28]. This provides evidence that the structural alterations of clusters may give rise to variations in the NLO properties [29]. More examples of heteroselenometallic cluster compounds will be synthesized for investigation of the structure/NLO property relationship.

Acknowledgements

This work was supported by the National Basic Research Program of China (973 Program, 2008CB617605) and the Program for New Century Excellent Talents in University

of China (NCET-06-0556). W.-H. Leung thanks the Hong Kong Research Grants Council (601506).

[1] Q. F. Zhang, W. H. Leung, X. Q. Xin, *Coord. Chem. Rev*. **2002**, *224*, 35.
[2] S. Shi, W. Ji, J. P. Lang, X. Q. Xin, *J. Phys. Chem*. **1994**, *98*, 3570.
[3] Q. F. Zhang, Y. N. Xiong, T. S. Lai, W. Ji, X. Q. Xin, *J. Phys. Chem. B* **2000**, *104*, 3476.
[4] Y. Xiong, Q. Zhang, X. Sun, W. Tan, X. Xin, W. Ji, *Appl. Phys. A* **2000**, *70*, 85.
[5] See any issue of *The Bulletin of the Selenium-Tellurium Development Association*, Grimbergen, Belgium.
[6] C. C. Christuk, M. A. Ansari, J. A. Ibers, *Inorg. Chem*. **1992**, *31*, 4365.
[7] C. C. Christuk, J. A. Ibers, *Inorg. Chem*. **1993**, *37*, 5105.
[8] R. J. Salm, J. A. Ibers, *Inorg. Chem*. **1994**, *33*, 4216.
[9] R. J. Salm, A. Misetic, J. A. Ibers, *Inorg. Chim. Acta* **1995**, *240*, 239.
[10] C. C. Christuk, M. A. Ansari, J. A. Ibers, *Angew. Chem*. **1992**, *104*, 1519; *Angew. Chem., Int. Ed. Engl*. **1992**, *31*, 1477.
[11] M. C. Hong, Q. F. Zhang, R. Cao, D. X. Wu, J. T. Chen, W. J. Zhang, H. Q. Liu, J. X. Lu, *Inorg. Chem*. **1997**, *36*, 6251.
[12] Q. F. Zhang, W. H. Leung, X. Q. Xin, H. K. Fun, *Inorg. Chem*. **2000**, *39*, 417.
[13] Q. F. Zhang, Y. Song, W. Y. Wong, W. H. Leung, X. Xin, *J. Chem. Soc., Dalton Trans*. **2002**, 1963.
[14] Q. F. Zhang, J. Ding, Z. Yu, Y. Song, A. Rothenberger, D. Fenske, W. H. Leung, *Inorg. Chem*. **2006**, *45*, 8638.
[15] S. Miao, Z. Yu, Q. F. Zhang, Y. Song, A. Rothenberger, W. H. Leung, *J. Cluster Sci*. **2006**, *17*, 495.
[16] Q. F. Zhang, Z. Yu, J. Ding, Y. Song, A. Rothenberger, D. Fenske, W. H. Leung, *Inorg. Chem*. **2006**, *45*, 5187.
[17] S. C. O'Neal, J. W. Kolis, *J. Am. Chem. Soc*. **1988**, *110*, 1971.
[18] SMART, SAINT+ for Windows NT (version 6.02a), Bruker Analytical X-ray Instruments Inc., Madison, Wisconsin (USA) **1998**.
[19] G. M. Sheldrick, SADABS, Program for Empirical Absorption Correction of Area Detector Data, University of Göttingen, Göttingen (Germany) **1996**.
[20] G. M. Sheldrick, SHELXTL (version 5.1), Software Reference Manual, Bruker AXS Inc., Madison, Wisconsin (USA) **1997**.
[21] M. Sheik-Bahae, A. A. Said, T. H. Wei, D. J. Hagan, E. W. Van Stryland, *IEEE J. Quantum. Electron*. **1990**, *26*, 760.
[22] Q. F. Zhang, R. Cao, M. C. Hong, D. X. Wu, W. J. Zhang, Y. Zheng, H. Q. Liu, *Inorg. Chim. Acta* **1998**, *271*, 93.
[23] Q. F. Zhang, W. H. Leung, Y. L. Song, M. C. Hong, C. L. Kennard, X. Q. Xin, *New J. Chem*. **2001**, *25*, 465.
[24] Q. F. Zhang, C. Zhang, Y. L. Song, X. Q. Xin, *J. Mol. Struct*. **2000**, *525*, 79.
[25] M. A. Ansari, C.-N. Chau, C. H. Mahler, J. A. Ibers, *Inorg. Chem*. **1989**, *28*, 650.
[26] A. Müller, E. Diemann, R. Jostes, H. Bögge, *Angew. Chem*. **1981**, *93*, 957; *Angew. Chem., Int. Ed. Engl*. **1981**, *20*, 934.
[27] H. W. Hou, X. Q. Xin, S. Shi, *Coord. Chem. Rev*. **1996**, *153*, 169.
[28] S. Shi, Z. Lin, Y. Mo, X. Q. Xin, *J. Phys. Chem*. **1996**, *100*, 10696.
[29] B. J. Coe, N. R. M. Curati, *Comments Inorg. Chem*. **2004**, *25*, 147.